A COMPREHENSIVE STUDY ON WASTE HEAT RECOVERY FROM INTERNAL COMBUSTION ENGINES USING ORGANIC RANKINE CYCLE

by

Mojtaba TAHANI [a, b], Saeed JAVAN [c*], and Mojtaba BIGLARI [c]

[a] Faculty of New Sciences and Technologies, Tehran University, Tehran, Iran
[b] Islamic Azad University, Center Tehran Branch, Tehran, Iran
[c] Department of Energy Conversion, Faculty of Mechanical Engineering, Semnan University, Semnan, Iran

Original scientific paper
DOI: 10.2298/TSCI111219051T

There are a substantial amount of waste heat through exhaust gas and coolant of an internal combustion engine. Organic Rankine cycle is one of the opportunities in internal combustion engines waste heat recovery. In this study, two different configurations of organic Rankine cycle with the capability of simultaneous waste heat recovery from exhaust gas and coolant of a 12 liter diesel engine were introduced: Preheat configuration and two-stage. First, a parametric optimization process was performed for both configurations considering R-134a, R-123, and R-245fa as the cycle working fluids. The main objective in optimization process was maximization of the power generation and cycle thermal efficiency. Expander inlet pressure and preheating temperature were selected as design parameters. Finally, parameters like hybrid generated power and reduction of fuel consumption were studied for both configurations in different engine speeds and full engine load. It was observed that using R-123 as the working fluid, the best performance in both configurations was obtained and as a result the 11.73% and 13.56% reduction in fuel consumption for both preheat and two-stage configurations were found, respectively.

Key words: *internal combustion engine, waste heat recovery, organic Rankine cycle, configuration, parametric optimization*

Introduction

Considering the climate change and the shortage of non-renewable energy resources, the interests in waste heat recovery has been growing remarkably, especially during the past decade [1, 2]. Waste heat recovery from internal combustion engines (ICE) is one of the opportunities for economizing of energy consumption. In an ICE, a great amount of fuel energy is wasted in form of heat due to thermal limitations. Roughly one-third of fuel energy is converted to mechanical power and the rest is released to the ambient in form of heat. For example, for a spark ignition 1.4 liter ICE with thermal efficiency of 15 to 32%, 1.7 to 45 kW of energy is wasted through coolant in radiator and 4.6 to 120 kW of energy is wasted by the exhaust gas [3]. Different methods have been recommended for waste heat recovery from ICE; such as thermoelectric, absorption refrigeration system, and organic Rankine cycle (ORC). For example in 2011 Ramesh Kumar *et al*. [4] have studied thermoelectric method in exhaust gas waste heat recovery

---

This paper belongs to No. 1, 2013, issue devoted to processes in internal combustion engines. From technical reasons we publish this paper in this issue.

* Corresponding author; e-mail: sa.javan67@gmail.com

of a three cylinder spark ignition engine through an experimental test. Waste heat recovery using ORC is an efficient method compared with the other techniques; so automobile manufacturers use this method to enhance the efficiency of their products [5-7]. In 2007, Hountalas *et al.* [8] investigated efficiency of a heavy diesel engine using the methods of heat recovery from exhaust gas. These methods include mechanical turbo compounding, electrical turbo compounding and steam Rankine cycle. In 2010 Farzaneh-Gord *et al*. [9] investigated heat recovery from a 1.7 liter natural gas powered internal combustion by CO_2 transcritical power cycle. Many researchers have been performed about using different working fluids, different configurations of Rankine cycle, and improving the system components during the recent years [10-16]. In 2009, Dai *et al*. [17] studied the effect of using different fluids on the heat recovery Rankine cycle and optimized the thermodynamic parameters like exergy efficiency for the studied working fluids. Vaja and Gambarotta [18] studied the effect of various working fluids on the efficiency of Rankine cycle used for waste heat recovery. Tahir *et al*. [19] investigated the effect of using Rotary-Vane Type expander on the efficiency of Rankine cycle used for waste heat recovery. Srinivasan *et al*. [20] examined the exhaust waste heat recovery potential of a high-efficiency, low-emissions dual fuel low temperature combustion engine using an ORC.

In this study, the various waste heat resources were investigated in a 12-liter compression ignition engine; then, two different configurations of Rankin cycle were introduced for simultaneous heat recovery from the studied engine coolant and exhaust gases: Preheat and two-stage configurations. A parametric optimization process was considered for each configuration. The objective functions used in optimization process were the power generation and the cycle thermal efficiency. The optimum conditions for all studied working fluids (R-134a, R-123, and R-245fa) and both configurations were investigated under engine speed of 1800 rpm and engine load of 100%. Finally, under optimum conditions parameters such as hybrid power generation and fuel consumption reduction were studied and compared for both configurations at the operating engine speeds (800 to 2100 rpm). It's worth to mention that the power generated by these systems converted to electricity and can be used to remove parasitic loads from the engine.

A program was developed in MATLAB software to perform computations needed in this study. This program was dynamically linked to engineering equation solver (EES) software to obtain the thermodynamic properties of fluids.

Table 1. Main engine characteristic

Parameter	Specification
Engine type (model)	6-Cylinder, Linear, (DC12 06)
Max. nominal power [kW]	310
Bore [mm]	127
Stroke [mm]	154
Compression ratio	18.5:1
Fuel LHV [$MJkg^{-1}$]	43
Exhaust gas temperature [°C]	388-565
Engine jacket temperature [°C]	80
Exhaust gas flow [kgs^{-1}]	0.13-0.49
Engine jacket flow [kgs^{-1}]	1.13-4.16

System description

ICE considered in the investigation

In this study, a commercial engine applied in vehicles was used for heat recovery. This is a 12-liter, compression ignition, six-cylinder engine with linear arrangement. The studies were performed with engine load of 100% and engine speeds of 800 to 2100 rpm that consumes gas oil. Its technical characteristics and the fuel specifications were presented in tab. 1.

Organic Rankine cycle

Considered configurations of Rankine cycle in the investigation

Using an adaptable configuration corresponding to the heat sources is one of the methods to improve the performance of co-generation system. Various configurations have been presented for heat recovery using ORC. Some of them are simple, preheat, and regenerated Rankine cycle. The amount of recovered heat and consequently cycle output power for these configurations depend on their characteristics. In this study two different configurations are proposed for simultaneous coolant and exhaust gas heat recovery: Preheat and two-stage configurations.

Preheat configuration. The first configuration presented in this paper was conventional preheat Rankine cycle. As shown in fig. 1, the working fluid pressure has increased through process 1-2, after that a preheater was used for waste heat recovery from the coolant. The working fluid was preheated in this heat exchanger (process 2-3) then, entered the evaporator and was converted to saturated vapor by absorbing heat from the exhaust gas (process 3-4). After that it entered the expander and generated mechanical power by expanding (process 4-5). As it will be shown in the following sections, due to working fluid mass flow rate limitation, this configuration is unable to absorb the total heat released by the coolant. Thus, an air-cooled heat exchanger should be used to reduce the temperature of coolant before returning the engine.

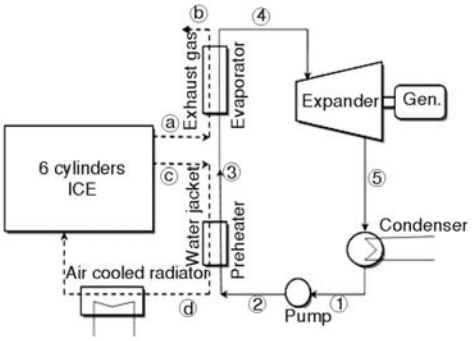

Figure 1. Preheat configuration combined with the ICE

Two-stage configuration. The second configuration is shown in fig. 2 it is the system rarely used for heat recovery from ICEs until now. Two pumps and one expander with two inlets and one outlet, usually called dual expander, were used in this system. As shown in this figure, in this configuration, the working fluid flows in two different stages with different pressures after leaving the condenser (process 1-2 and 1-3). Low pressure stage relates to heat recovery from the coolant (process 2-4) and another one relates to heat recovery from exhaust gas (process 3-5). Finally, both low and high pressure flows expanded through a dual expander (process 4 an 5-6). Using this configuration, total wasted heat of coolant can be recovered and there is no need to air-cooled heat exchanger for coolant. Using two-stage configuration for Rankin cycle named as "dual pressure steam cycle" was recommended by Wang *et al*. [21] in 2009 for heat recovery from a cement production factory. They used a dual steam turbine for compression and power generation stage.

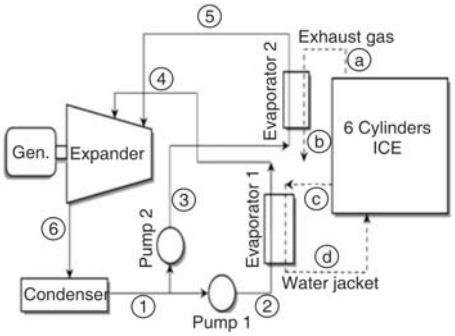

Figure 2. Two-stage configuration combined with the ICE

Selection of the working fluid

The fluids were categorized based on the slope of their saturation vapor line in *T-s* diagram into three groups: Wet fluids with positive slope

of saturation vapor line, dry fluids with negative slope of saturation vapor line, and isentropic fluids with an approximately vertical saturation vapor line. The wet fluid leads to droplets at the later stages of expander and requires superheating at the turbine inlet whereas the dry fluids are superheated even after the expansion from the expander. For an isentropic fluid, having a near-vertical saturated vapor line, the saturated vapor remains in the saturated condition and liquid droplets are not formed during expansion in expander. In an ORC utilizing this type of fluid under operation, most of the heat addition and rejection is carried out during change of phase only without the need of regenerative systems and it makes the ORC system a simpler one [22].

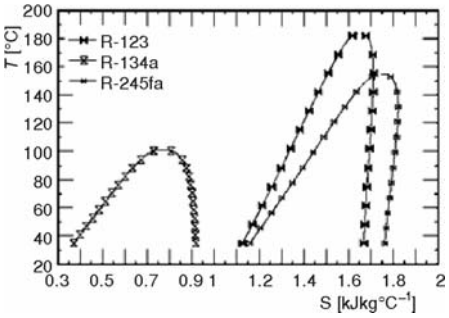

Figure 3. *T-s* diagram for considered working fluids

Based on the thermodynamic and environmental criteria for working fluid selection, R-134a was selected as the wet working fluid, R-123 was selected as the dry working fluid, and R-245fa was selected as the isentropic working fluid. *T-s* diagram for the mentioned fluids was shown in fig. 3 their characteristics are tabulated in tab. 2.

Table 2. Physical and thermodynamic data for considered working fluids

Parameter	Value		
Working fluid	R-134a	R-123	R-245fa
Chemical formula	CF_3CH_2F	$C_2HCl_2F_3$	$C_3H_3F_5$
Type	Wet	Dry	Isentropic
Critical temperature [°C]	101	183.7	154
Critical pressure [Mpa]	4.054	3.662	464.1
Ozone depleting potential	0.000	0.012	0.000
Global warming potential	1300	120	950
Flammability	Non-flammable	Non-flammable	Non-flammable

Thermodynamic analysis

To study the considered cycles some assumptions are applied:

– the isentropic efficiency of expanders and pumps are assumed to be 80% [23],
– the condenser temperature is assumed to be 35 °C,
– heat loss in the heat exchangers is assumed to be negligible,
– pressure drop in the heat exchangers and pipes are assumed to be negligible, and
– the electric generator efficiency is assumed to be 95% [18].

Generated power and thermal efficiency

Preheat configuration

As shown in fig. 1, in this configuration, the heat of the coolant was used to preheat the working fluid. Applying energy balance for preheater, required mass flow rate of working fluid was computed as follows:

$$\dot{m}_{\mathrm{wf1}} = \frac{\dot{Q}_{\mathrm{clnt}}}{h_3 - h_2} \tag{1}$$

Also as shown in fig. 1, an evaporator was used to absorb the wasted heat from exhaust gas. Mass flow rate of working fluid for heat recovery from exhaust gas was obtained from:

$$\dot{m}_{\mathrm{wf2}} = \frac{\dot{m}_{\mathrm{exh}} \overline{C}_{p\,\mathrm{exp}} (T_{\mathrm{a}} - T_{\mathrm{b}})}{h_4 - h_3} \tag{2}$$

In the eq. (2), T_{b} denotes exhaust gas temperature after heat recovery, in the both pre-heat and two-stage configurations, it was assumed to be 100 °C. Referring to the eqs. (1) and (2), the mass flow rate of working fluid for heat recovery from coolant ($\dot{m}_{\mathrm{wf1}}$) is noticeably greater than the corresponding value to absorb heat from exhaust gas ($\dot{m}_{\mathrm{wf2}}$). Mass flow rate of working fluid ($\dot{m}_{\mathrm{wf}}$) was considered as the minimum of these two. Thus, there is a mass flow rate limitation for complete heat recovery from coolant.

The recovered heat values from coolant and exhaust gas are given by:

$$\dot{Q}_{\mathrm{cln\ trec}} = \dot{m}_{\mathrm{cf}} \overline{C}_{p\,\mathrm{cf}} (T_c - T_d) \tag{3}$$

$$\dot{Q}_{\mathrm{ex\ hrec}} = \dot{m}_{\mathrm{exh}} \overline{C}_{p\,\mathrm{exh}} (T_{\mathrm{a}} - T_{\mathrm{b}}) \tag{4}$$

By applying an energy balance for the expander, the generated power was computed as follows:

$$\dot{W}_{\mathrm{exp\,ac}} = \eta_{\mathrm{exp}} \dot{m}_{\mathrm{wf}} (h_4 - h_{5\mathrm{s}}) \tag{5}$$

In eq. (5), denotes isentropic efficiency of expander and was assumed to be 80%.

The 1st law of thermodynamics efficiency was computed from:

$$\eta_{1^{st}\,law} = \frac{\dot{W}_{\mathrm{exp}}}{\dot{Q}_{\mathrm{exh\ rec}} + Q_{\mathrm{clnt\ rec}}} \tag{6}$$

Two-stage configuration

In two-stage Rankine cycle, each stage absorbs heat from one of the two hot sources independently. Thus, there is no problem about mass flow rate limitation. The required mass flow rate of working fluid in the first stage is given as:

$$\dot{m}_{\mathrm{wf1}} = \frac{\dot{m}_{\mathrm{cf}} \overline{C}_{p\,\mathrm{cf}} (T_c - T_d)}{h_4 - h_2} \tag{7}$$

The second stage of this configuration recovers the exhaust gas heat. Applying the energy balance, required mass flow rate for the second stage is given as:

$$\dot{m}_{\mathrm{wf2}} = \frac{\dot{m}_{exh} \overline{C}_{p\,\mathrm{exh}} (T_{\mathrm{a}} - T_{\mathrm{b}})}{h_5 - h_3} \tag{8}$$

Dual expander was employed to generate mechanical power in this configuration. The generated power by this configuration was computed by applying 1st law of thermodynamics for expander with two inlets and one outlet:

$$\dot{W}_{\mathrm{exp\,ac}} = \eta_{\mathrm{exp}} [\dot{m}_{\mathrm{wf1}} (h_4 - h_{6\mathrm{s}}) + \dot{m}_{\mathrm{wf2}} (h_5 - h_{6\mathrm{s}})] \tag{9}$$

The expander isentropic efficiency (η_{exp}) was also considered as 80%.

The 1st law of thermodynamics efficiency for two-stage cycle was calculated from:

$$\eta_{1^{st}_{\text{law}}} = \frac{\dot{W}_{\text{exp ac}}}{\dot{Q}_{\text{exh rec}} + Q_{\text{clnt}}} \tag{10}$$

Heat exchanger effectiveness

Effectiveness concept can be used to evaluate heat exchangers; which is defined as the ratio of actual heat transfer rate in a heat exchanger to the thermodynamically limited possible heat transfer rate in a counter flow heat exchanger.

Maximum heat transfer rate and also heat exchanger effectiveness are given by [24]:

$$\dot{Q}_{\text{max.}} = (\dot{m} C_p)_{\text{min.}} (T_{\text{h,i}} - T_{\text{c,i}}) \tag{11}$$

$$\varepsilon = \frac{\dot{Q}}{\dot{Q}_{\text{max.}}} \tag{12}$$

Named as heat capacity rate, $\dot{m}C_p$, which in eq. (11) has its minimum amount between hot flow in heat exchange with cold flow.

Engine thermal efficiency and fuel consumption

One of the benefits of co-generation using ORC is the enhancement of engine thermal efficiency. Equations (11) and (12) were used to determine the engine thermal efficiency and in the case of engine bottoming with ORC, respectively, [25]:

$$Eff_{\text{Eng}} = \frac{Eng\ power}{\dot{m}_{\text{f}} \times \text{LHV}} \tag{13}$$

$$Eff_{\text{Eng-ORC}} = \left(\frac{Eng\ power + ORC\ power}{\dot{m}_{\text{f}} LHV} \right) \tag{14}$$

where LHV denotes lower heating value of the fuel considered as 43 MJ/kg. The fuel reduction percentage (FRP) was calculated from:

$$FRP = \left[1 - \frac{Eff_{\text{Eng}}}{Eff_{\text{Eng-ORC}}} \right] \cdot 100 \tag{15}$$

Thus, the reduction percentage of fuel consumption can be estimated for both configurations.

Parametric optimization

To compare two studied configurations, they have to operate under the best thermodynamic conditions. For this reason, a parametric optimization process was applied for both configurations and all considered fluids. The effects of the expander inlet pressure and the preheating value on the power generation and thermal efficiency were investigated when the expander inlet working fluid was a saturated vapor.

In two-stage configuration, due to different fluid pressures at expander inlets, the stages were optimized by separate processes. In preheat configuration, the optimum temperature of working fluid at preheater outlet should be investigated in addition to find the optimum conditions at the expander inlet. So the system was first investigated without preheater to find the optimum pressure value. After finding the optimum value of expander inlet pressure, the optimum value of working fluid temperature at the preheater outlet was investigated. Enhancing the

first stage pressure of two-stage configuration was performed during 100 steps from the condenser pressure to the corresponding pressure with the saturation temperature of working fluid while it is at the same temperature of engine outlet coolant fluid. Enhancing the second stage pressure was also performed during 100 steps from the first stage maximum possible temperature to the critical pressure of studied fluid. In preheat cycle; there is no need to find the expander optimum inlet pressure, because its conditions are similar to the conditions of the second stage of two-stage cycle. Thus, the optimum pressure is known for all fluids, and only the working fluid temperature at the preheater outlet should be investigated. It's noticeable that some limiting conditions were considered during optimization process. These constraints are presented in the following:

– the maximum expansion ratio of expander was assumed as 20. Increasing the expansion ratio of expanders increases and then decreases their efficiency; so that for expansion ratio of 20, the efficiency usually has its maximum value equal to 80%,
– the maximum effectiveness of heat exchangers used for heat absorption was considered as 80%. In heat exchangers, the required area for heat exchange increases with increasing the exchanger effectiveness; so that up to effectiveness of 80%, the required area for heat exchange increases almost linearly with the effectiveness, thereafter, a little increment in effectiveness results in a noticeable increment in the required area for heat exchange [26], and
– the minimum value of steam quality at the expander outlet was assumed as 90%. The excessive reduction in steam quality and liquid drops formation at the expander outlet inflicts a serious damage to the expander blades.

The mentioned constraints were tabulated in tab. 3.

Table 3. The list of constraints for optimization

Constraint	Value
Maximum expansion ratio [–]	20
Maximum heat exchanger effectiveness [%]	80
Minimum vapor quality [%]	90

Discussion and results

Two-stage configuration

The effect of first stage pressure on produced power and thermal efficiency

The resultant optimum pressure values of R-134a, R-123, and R-245fa at the first stage were presented in figs. 4 to 6, respectively. Also, effectiveness of the heat exchanger used in the cycle first stage was shown *vs.* the first stage pressure for all three working fluids in fig. 7. About the effect of cycle pressure on heat exchangers effectiveness, it is worth to mention that by increment of expander inlet pressure, saturation temperature is increased; so actual transferred heat in heat exchanger is increased, however maximum transferred heat is fixed and as a result heat exchanger effectiveness is increased by pressure increment.

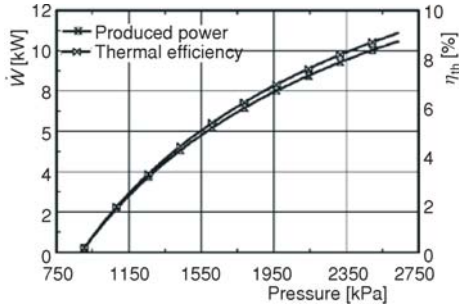

Figure 4. Produced power and thermal efficiency *vs.* first stage pressure for R-134a

As shown in fig. 4, for R-134a, increasing the first stage pressure always increases both values of produced power and thermal efficiency. Thus, the optimum pressure value for the first stage corresponding with the maximum work and thermal efficiency was 2.5 MPa. As mentioned before, the heat exchangers effectiveness should not exceed 0.8 during the optimization

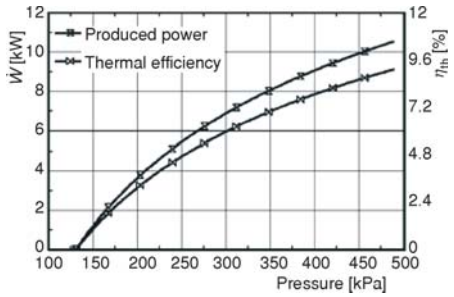

Figure 5. Produced power and thermal efficiency *vs.* first stage pressure for R-123

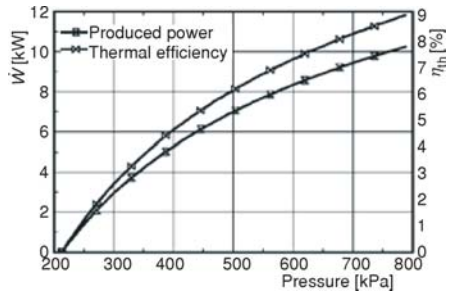

Figure 6. Produced power and thermal efficiency *vs.* first stage pressure for R-245fa

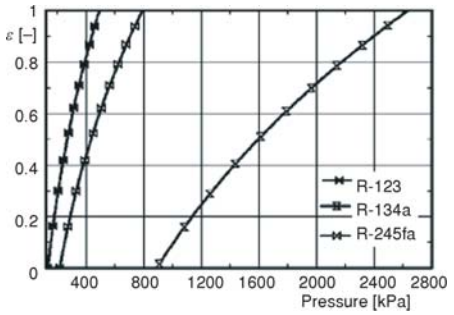

Figure 7. First stage heat exchanger effectiveness *vs.* pressure

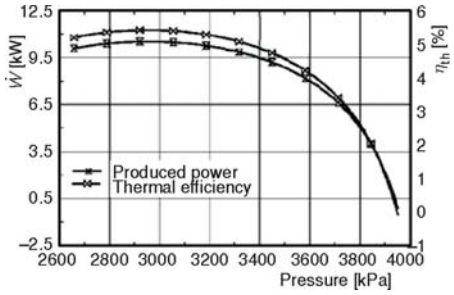

Figure 8. Produced power and thermal efficiency *vs.* second stage pressure for R-134a

process. As shown in fig. 7, corresponding pressure with this value of effectiveness was 2.1 MPa. Thus, the favorable conditions of the first stage with R-134a as the working fluid will be obtained at the pressure of 2.1 MPa. At this pressure, the values of power generation and thermal efficiency were 8.83 kW and 7.6%, respectively.

Figure 5 shows the effect of enhancing the first stage pressure on the power generation and thermal efficiency for R-123. For this fluid, the optimum value of the first stage pressure was 0.5 MPa to obtain maximum power and efficiency. Referring to fig. 7 and investigating the heat exchanger effectiveness for this fluid show that this parameter exceeded the allowable value. Thus, the favorable pressure should be changed to 0.38 MPa. At this pressure, the power generation and thermal efficiency are 8.84 kW and 7.65%, respectively.

Figure 6 shows the effect of enhancing the first stage pressure on the power generation and thermal efficiency for R-245fa. For this fluid, the pressure values corresponding with the maximum power generation and thermal efficiency are the same, and they are equal to the maximum possible pressure for the first stage, *i. e.* 0.78 MPa. By investigating the evaporator effectiveness shown in fig. 7, the optimum pressure for this fluid decreases to 0.62 MPa. The maximum power generation and thermal efficiency for this fluid were 8.6 kW and 7.5%, respectively.

It was found from the results that the values of power generation and thermal efficiency resulted from optimization based on the first stage pressure are approximately the same for the three fluids. The optimum pressure value computed for R-134a is greater than the other two fluids; and thus, the maintenance costs of system for this fluid are greater than the two other fluids.

The effect of second stage pressure on produced power and thermal efficiency

The results obtained for R-134a, R-123, and R-245fa were shown in figs. 8 to 11, respectively. Also, the effects of enhancing pressure on heat exchanger effectiveness, expander expansion ratio, and the steam quality at expander outlet were illustrated in figs. 12 to 14, respectively.

The effects of enhancing the second stage pressure on power generation and thermal efficiency for R-134a were shown in fig. 8. The variations rate of the mentioned two parameters with pressure was illustrated in fig. 9 to obtain a better understanding about their variations with pressure. As shown in this figure, the variations rate is positive up to 2.9 MPa; at this pressure, it is zero; and thereafter it is negative. Thus, both parameters have their maximum value at 2.9 MPa. All constraints are satisfied at this pressure. This is evident referring to fig. 12 for heat exchanger effectiveness, fig. 13 for expander expansion ratio, and fig. 14 for outlet steam quality. At this pressure, the generated work and thermal efficiency of the second stage are 10.51 kW and 5.4%, respectively.

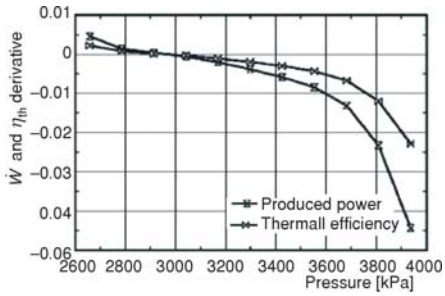

Figure 9. Variation rate of produced power and thermal efficiency *vs.* second stage pressure for R-134a

The effect of enhancing the second stage pressure for R-123 was shown in fig. 10. As shown in this figure, the power and thermal efficiency increase and then decrease with pressure. The pressure corresponding with the maximum power and efficiency was 2.6 MPa. Referring to limiting values presented in figs. 12 to 14, it is observed that the heat exchanger effectiveness is in allowable range. Also, the problem of liquid drops formation at the expander outlet was solved using dry fluid, but the expander expansion ratio exceeded its limit value. Thus, the second stage pressure should decrease to 2.23 MPa. At this pressure, the optimum values of generated work and thermal efficiency are 40.54 kW and 21%, respectively.

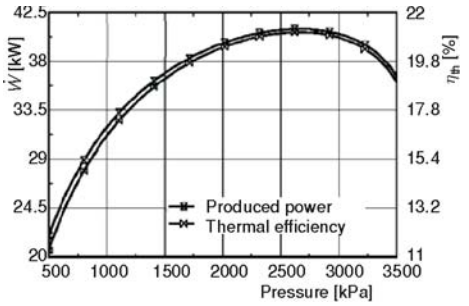

Figure 10. Produced power and thermal efficiency *vs.* second stage pressure for R-123

Figure 11 shows the values of work and efficiency for R-245fa. With this working fluid, the generated power and thermal efficiency increase and then decrease with pressure. The maximum value of the mentioned parameters occurred at 2.6 MPa. The values of all three limiting factors were within their allowable range. The maximum generated power and thermal efficiency were 36.2 kW and 18.25%, respectively.

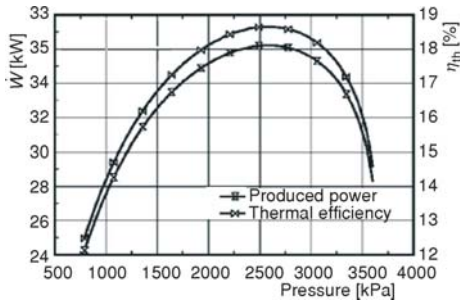

Figure 11. Produced power and thermal efficiency *vs.* second stage pressure for R-245fa

The ultimate results obtained from the optimization of two-stage cycle were tabulated in tab. 4. As observed in this table, the maximum values of power generation and thermal efficiency were obtained with R-123, and the minimum values of mentioned parameters were obtained with R-134a as the working fluid. Moreover, R-134a needs a higher mass flow rate of working fluid, higher operating pressure, and higher power consumption of pumps in comparison with the other two working fluids. Thus, it's not a good choice for the cycle working fluid. Also, between R-245fa and R-123, the latter has lower operating pressure, higher power

Table 4. The optimization results of two-stage cycle for considered working fluids

Parameter	R-134a		R-123		R-245fa	
	1st stage	2nd stage	1st stage	2nd stage	1st stage	2nd stage
Condenser temperature [°C]	35		35		35	
Expander inlet pressure [MPa]	2.1	2.9	0.38	2.2	0.62	2.6
Mass flow rate [kgs^{-1}]	0.65	1.1	0.61	0.84	0.54	0.78
Feed pump consumption [kW]	0.7	1.9	0.10	1.27	0.19	2.11
Produced power [kW]	19.34		49.38		44.80	
Thermal efficiency [%]	6.22		15.69		14.40	

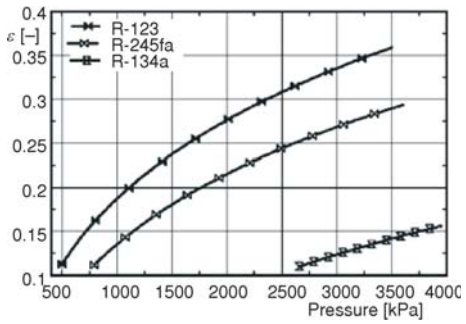

Figure 12. Second stage heat exchanger effectiveness *vs.* pressure

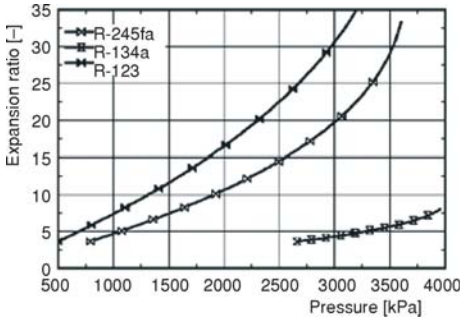

Figure 13. Expansion ratio of expander *vs.* pressure

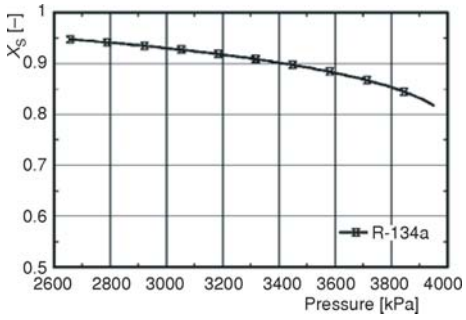

Figure 14. Quality of vapor at outlet of expander *vs.* pressure

generation and thermal efficiency, and lower pump consumption; and thus, it's a better option as the working fluid of two-stage cycle.

Preheat configuration

The effect of preheating on produced power and thermal efficiency

Figures 15 to 17 show the effect of working fluid temperature at the preheater outlet on power generation and thermal efficiency for R-134a, R-123, and R245fa, respectively. Also, fig. 18 shows the effect of working fluid temperature at the preheater outlet on preheater effectiveness for these fluids.

Figure 15 shows the effect of increasing the temperature of preheated working fluid on the generated power and thermal efficiency for R-134a. As it shown, by increasing temperature of preheating the produced power and thermal efficiency increases and remains constant, respectively. The maximum generated power was 28.71 kW with the working fluid temperature of 80 °C at the end of preheating. Due to the preheater effectiveness value shown in fig. 18, it was found that the maximum preheating temperature was limited to 71.11 °C. Thus, the maximum generated power decreased to 25.2 kW, but thermal efficiency remained constant.

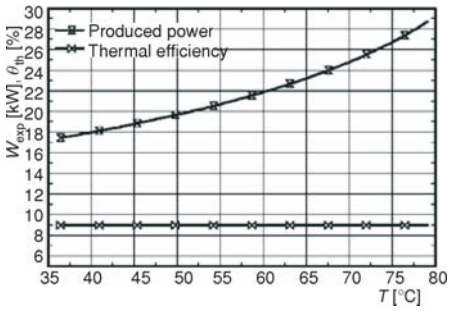

Figure 15. Produced power and thermal efficiency *vs.* temperature of preheated working fluid for R-134a

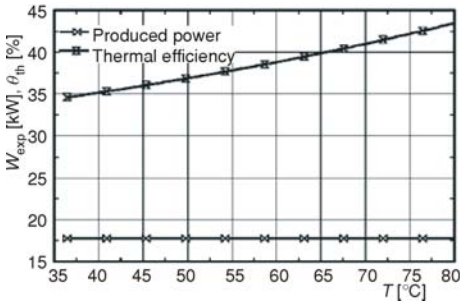

Figure 16. Produced power and thermal efficiency *vs.* temperature of preheated working fluid for R-123

Figure 16 shows the effect of increasing the temperature of preheated working fluid on the generated power and thermal efficiency for R-123. As expected, increasing the preheated fluid temperature increased the generated power. The maximum generated power was 43.5 kW with the working fluid temperature of 80 °C at the preheater outlet; *i. e.* when the outlet working fluid was at the same temperature with the preheater inlet coolant fluid. But the preheater efficiency increases with the preheated fluid temperature. It was found, from fig. 18, that the maximum preheated temperature of the mentioned liquid considering the allowable value of preheater effectiveness was 71 °C. At this temperature which is the optimum temperature for preheated liquid, the values of generated power and cycle thermal efficiency were 41.25 kW and 17.76%, respectively.

Figure 17 shows the effect of preheating on the generated power and thermal efficiency for R-245fa. For this liquid, the variations trends of generated power and thermal efficiency with increasing the preheated working fluid temperature were strictly--increasing and constant, respectively. Thus, the maximum generated power was 39 kW corresponding with constant thermal efficiency value of 14.8%. Referring to the preheater effectiveness value shown in fig. 18, it was found that the maximum preheating temperature was limited to 70.6 °C. Thus, the maximum generated power decreased to 36.26 kW, but thermal efficiency remained constant.

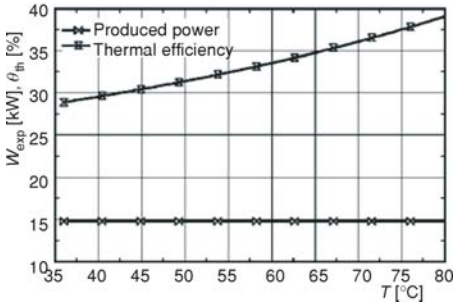

Figure 17. Produced power and thermal efficiency *vs.* temperature of preheated working fluid for R-245fa

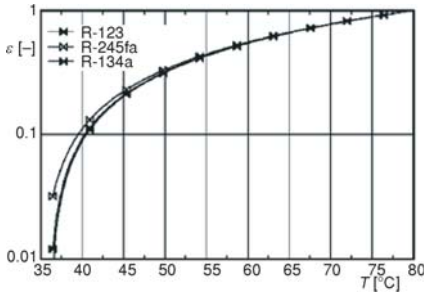

Figure 18. Preheater effectiveness *vs.* temperature

The results of optimizing the preheat configuration for the fluid temperature at preheater outlet were summarized in tab. 5 for R-134a, R-123, and R245fa. As observed in this table for preheat configuration, the highest power generation and thermal efficiency, and also the lowest required pumping power were related to R-123. Referring to tabs. 4 and 5 and comparing each fluid in both configurations, it was found that with R-134a as the working fluid, preheat configuration has better performance than two-stage configuration in the view of

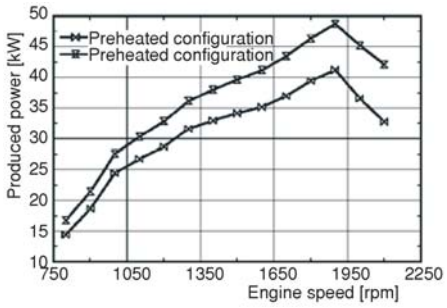

Figure 19. The output power and fuel reduction percentage of both configurations *vs.* the engine speed

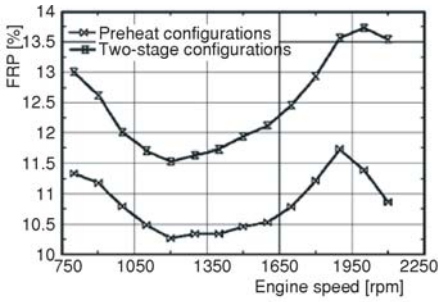

Figure 20. The reduction percentages of fuel consumption for both configurations *vs.* the engine speed

Table 5. The optimization results of preheat cycle for considered working fluids

Parameter	R-134a	R-123	R-245fa
Condenser temperature [°C]	35	35	35
Preheater outlet temperature [°C]	71.11	71.00	70.06
Mass flow rate [kgs^{-1}]	1.58	1.01	0.98
Feed pump consumption [kW]	2.3	1.734	2.69
Produced power [kW]	25.2	41.25	36.26

power generation and thermal efficiency. Applying preheat configuration also necessitates using less equipment. But with using the other two fluids, two-stage configuration has priority over preheat configuration in the view of power generation.

Hybrid produced power and reduction of fuel consumption

R-123 was used to investigate the hybrid power generation and fuel consumption reduction of the studied engine caused by applying both configurations with their operating engine speeds under full load; and the results were presented. The output power of both configurations versus the engine speed was shown in fig. 19. It was observed that at the same engine speeds, the output power of two-stage system was greater than preheat configuration, and this difference increases with increasing the engine speed.

One of the results of co-generation is to economize in the fuel consumption. The reduction percentages of fuel consumption for both configurations were shown in fig. 20. In both configurations, the greatest reduction of fuel consumption occurred at engine speeds of 1900 and 800 rpm, respectively.

Conclusions

In this paper, the amount of wasted heat from different parts of a 12 liter compression ignition engine and their potential for waste heat recovery were investigated. Then, two configurations were introduced for simultaneous heat recovery from exhaust gases and coolant. An optimization process was applied for the configurations in which the goal was to maximize the work generation and thermal efficiency for three different working fluids. It was found that in both cycles, the best performance was obtained when R-123 was applied as the working fluid. Also, it was observed that in the case of using R-134a as the working fluid in both configurations, the preheat configuration has better results. Although due to the mass flow rate limitation of working fluid, preheat configuration was unable to recover total wasted heat from coolant.

Therefore, an air-cooled heat exchanger was required for coolant. Although, two-stage cycle absorbed the total heat of coolant; so the air-cooled heat exchanger was eliminated. Moreover, two-stage cycle generated 49.38 kW of mechanical power which was 16.4% greater than the corresponding value of preheat cycle (41.25 kW). The decrement of reduction of fuel consumption was also studied, as a consequent of using these systems for co-generation resulted in 11.73 and 13.56% reduction in fuel consumption.

Acknowledgment

The authors gratefully acknowledge supports of the talented office of Semnan University for funding the current research grant and also the collaboration of Oghab Afshan Industrial & Manufacturing Co. for preparing engine technical data; especially Dr. Abbas Honarbakhsh Raouf.

Nomenclature

C_p – specific heat at constant pressure, [kJkg^{-1}K^{-1}]
h – specific enthalpy [kJkg^{-1}]
$\dot{m}$ – mass flow rate [kgs^{-1}]
Q – heat transfer rate [kW]
T – temperature [°C]
$\dot{W}$ – power [kW]
X_s – vapor quality at the end of expander, [–]

Greek symbols

η – efficiency [%]
ε – heat exchanger effectiveness [%]

Subscripts

amb – ambient
c – cold
cf – cooling fluid
Eff – engine thermal efficiency
Eng – engine
Eng-Orc – engine-organic Rankine cycle
exh – exhaust gas
exp – expander
f – fuel
h – hot
i – inlet
max. – maximum
min. – minimum
rec – recovered
th – thermal
wt – thermal
wf – working fluid

Acronyms

ICE – internal combustion engine
rpm – round per minute (engine speed)
LHV – low heating value
ORC – organic Rankine cycle

References

[1] Ravikumar, N., *et al*., Thermodynamic Analysis of Heat Recovery Steam Generator in Combined Cycle Power Plant, *Thermal Science, 11* (2007), 4, pp. 143-156
[2] Polyzakis, A. L., *et al*., Long-Term Optimization Case Studies for Combined Heat and Power System, *Thermal Science, 13* (2009), 4, pp. 46-60
[3] Chammas, El., Clodic, R., Clodic, D., Combined Cycle for Hybrid Vehicles, SAE paper No. (2005)-01-1171, 2005
[4] Ramesh Kumar, C., *et al*., Experimental Study on Waste Heat Recovery from an IC Engine Using Thermoelectric Technology, *Thermal Science*, *16* (2011), 4, pp. 1011-1022
[5] Zhang, H., *et al*., Study of Parameters Optimization of ORC for Engine Waste Heat Recovery, *Adv Mat Res*, *201-203* (2011), pp. 585-589
[6] Kadota, M., Yamamoto, K., Advanced Transient Simulation on Hybrid Vehicle Using Rankine Cycle System, SAE paper 2008-01-0310, 2008
[7] Ringler, J., *et al*., Rankine Cycle for Waste Heat Recovery of IC Engines, SAE paper 2009-01-0174, 2009
[8] Hountalas, D. T., *et al*., Study of Available Exhaust Gas Heat Recovery Technologies for HD Diesel Engine Applications, *Int. J. Altern Propul, 1* (2007), 2/3, pp. 228-249
[9] Farzaneh-Gord, M., *et al*., Heat Recovery from a Natural Gas Powered Internal Combustion Engine by CO_2 Transcritical Power Cycle, *Thermal Science, 14* (2011), 4, pp. 897-911
[10] Endo, T., *et al*., Study on Maximizing Exergy in Automotive Engines, SAE paper 2007-01-0257, 2007

[11] Saleh, B., *et al*., Working Fluids for Low-Temperature Organic Rankine Cycles, *Energy, 32* (2007), 7, pp. 1210-1221
[12] Wei, D., *et al*., Dynamic Modeling and Simulation of an Organic Rankine Cycle System for Waste Heat Recovery, *Appl. Therm. Eng., 28* (2008), 10, pp. 1216-1224
[13] Wipplinger, K. P. M., *et al*., Stainless Steel Finned Tube Heat Exchanger Design for Waste Heat Recovery, *J. of Energy in Southern Africa, 17* (2006), 2, pp. 47-56
[14] Drescher, U., Bruggermann, D., Fluid Selection for the Organic Rankine Cycle in Biomass Power and Heat Plants, *Appl. Therm. Eng., 27* (2007), 1, pp. 223-228
[15] Maizza, V., Maizza, A., Unconventional Working Fluids in Organic Rankine Cycles for Waste Heat Recovery Systems, *Appl. Therm. Eng., 21* (2001), 3, pp. 381-390
[16] Mago, P. J., *et al*., An Examination of Regenerative Organic Rankine Cycles Using Dry Fluids, *Appl. Therm. Eng., 28* (2008), 8-9, pp. 998-1007
[17] Dai, Y., *et al*., Parametric Optimization and Comparative Study of Organic Rankine Cycle for Low Grade Waste Heat Recovery, *Energy Convers. Manage., 50* (2009), 3, pp. 576-582
[18] Vaja, I., Gambarotta, A., Internal Combustion Engine (ICE) Bottoming with Organic Rankine Cycles, *Energy, 35* (2010), 2, pp. 1084-1093
[19] Tahir, M. B. M., *et al*., Efficiency of Organic Rankine Cycle System with Rotary-Vane- Type Expander for Low-Temperature Waste Heat Recovery, *Inter. Jour. of Civil and Environmental Engineering, 2* (2010), 1, pp. 11-16
[20] Srinivasan, K. K., *et al*., Analysis of Exhaust Waste Heat Recovery from a Dual Fuel Low Temperature Combustion Engine Using an Organic Rankine Cycle, *Energy, 35* (2010), 6, pp. 2387-2399
[21] Wang, J., *et al*., Exergy Analyses and Parametric Optimizations for Different Cogeneration Power Plants in Cement Industry, *Appl. Energy, 86* (2009), 6, pp. 941-948
[22] Roy, J. P., *et al*., Parametric Optimization and Performance Analysis of a Waste Heat Recovery System Using Organic Rankine Cycle, *Energy*, *35* (2010), 12, pp. 5049-5062
[23] Drescher, U., Bruggermann, D., Fluid Selection for the Organic Rankine Cycle in Biomass Power and Heat Plants, *Appl. Therm. Eng, 27* (2007), 1, pp. 223-228
[24] Incroprera, F. P., De Witt, D. P., *Fundamentals of Heat and Mass Transfer*, John Wiley & Sons, New York, USA, 2001
[25] Tantiworrawit, P., Heat Recovery from Diesel Engines in Vehicles by Using Rankine Cycles for Power Production, Master's thesis, Chalmers University of Technology, Goteborg, Sweden, 2010
[26] Kakac, S., Liu, H., *Heat Exchanger Selection, Rating and Thermal Design*, 2nd ed., CRC Press, Taylor & Francis Group, New York, USA, 2002

Paper submitted: December 19, 2011
Paper revised: February 6, 2012
Paper accepted: April 1, 2012